

PSFC/JA-03-11

**Observations of Anomalous Transport in Tokamak
Plasmas with No Momentum Input**

W.D. Lee, J.E. Rice, E.S. Marmor, M.J. Greenwald,
I.H. Hutchinson, J.A. Snipes

May 2003

Plasma Science and Fusion Center
Massachusetts Institute of Technology
Cambridge, MA 02139 USA

This work was supported by the U.S. Department of Energy, Cooperative Grant No. DE-FC02-99ER54512. Reproduction, translation, publication, use and disposal, in whole or in part, by or for the United States government is permitted.

Submitted for publication to *Phys. Rev. Letters*.

Observations of Anomalous Momentum Transport in Tokamak Plasmas with No Momentum Input

W. D. Lee, J. E. Rice, E. S. Marmor, M. J. Greenwald, I. H. Hutchinson and J. A. Snipes
Plasma Science and Fusion Center, MIT, Cambridge, MA 02139-4307

Abstract

Anomalous momentum transport has been observed in Alcator C-Mod tokamak plasmas. The time evolution of core impurity toroidal rotation velocity profiles has been measured with a crystal x-ray spectrometer array. Following the L-mode to EDA (enhanced D_α) H-mode transition in both Ohmic and ICRF heated discharges, the ensuing co-current toroidal rotation velocity, which is generated in the absence of any external momentum source, is observed to propagate in from the edge plasma to the core with a time scale of order of the observed energy confinement time, but much less than the neo-classical momentum confinement time. The steady state toroidal rotation velocity profiles in EDA H-mode plasmas are relatively flat and the momentum transport can be simulated with a simple diffusion model. Assuming the L-H transition produces an instantaneous edge velocity source (which disappears at the H- to L-mode transition), the momentum transport may be characterized by a diffusivity, with values of $\sim 0.07 \text{ m}^2/\text{s}$ during EDA H-mode and $\sim 0.2 \text{ m}^2/\text{s}$ in L-mode. These values are large compared to the calculated neo-classical momentum diffusivities. Velocity profiles during ELM-free H-modes are centrally peaked, which suggests inward momentum convection; the observed profiles are matched with simulations including an inward convection velocity of $\sim 10 \text{ m/s}$. In EDA H-mode discharges which develop internal transport barriers, the velocity profiles become hollow in the center indicating the presence of a negative radial electric field well in the vicinity of the barrier foot.

Rotation and velocity shear play important roles in the transition to high confinement mode (H-mode) [1-4] and in the formation of internal transport barriers (ITBs) [5] in tokamak discharges. Compared to energy and particle transport, however, there has been considerably less effort addressing momentum transport. In a majority of tokamak plasmas, the observed toroidal rotation is generated externally by neutral beam injection. By measuring the rotation profiles from the associated beam diagnostics, and calculating the input torque profiles from the beam injection, momentum transport may be characterized [6-13]. Momentum confinement is generally found to be anomalous, with a diffusivity, χ_ϕ , similar to the ion thermal conductivity, χ_i [6-13], but much larger than the neo-classical diffusivity (viscosity). The reliability of this type of analysis relies on the accuracy of the input torque calculations, and the inherent assumption that there is no additional source of momentum when the plasma enters H-mode. Alcator C-Mod ICRF [14] and Ohmic [15] H-mode discharges are found to have substantial spontaneous co-current toroidal impurity rotation (as high as 100 km/s, Mach number 0.3) in spite of the fact that there is no momentum input. Similar observations have been made on other devices such as JET [16], COMPASS [17] and Tore Supra [18]. Several attempts to explain the observed rotation in C-Mod have been made, based on ICRF wave driven fast particle orbit shift mechanisms [19-20], turbulence [21-22] and sub-neo-classical [23] effects. The similarity of the rotation observed in ICRF and purely Ohmic plasmas suggests that it is not due to ICRF wave or fast particle effects. The prediction of reversal of the rotation direction with high magnetic field side (HFS) off-axis ICRF absorption [19-20] has not been observed in the experiments [24]. For the turbulence driven theories [21-22], the sign of the rotation is correct, but the magnitude cannot be tested because the turbulence fluctuation levels are not measured. The predictions of the rotation magnitude and direction from the sub-neo-classical theory agree with the measurements [23], but the calculated momentum diffusion time scale is two orders of magnitude longer than what is observed. In order to gain a better understanding of the mechanism generating the rotation in the absence of an external source, and in general to characterize momentum transport, temporally resolved velocity profiles are needed. Previous off-axis measurements of the doppler shifts of argon x-ray lines on Alcator C-Mod were along sightlines with only a slight toroidal component [14], so only large rotation velocities could be seen, and only then with poor time resolution. The Alcator C-Mod x-ray crystal spectrometer system has now been modified with three fully tangential views, at $r/a = 0.0, 0.3$ and 0.6 . These three rotation measurements are augmented by the velocity of magnetic perturbations associated with sawtooth oscillations recorded with an array of fast pickup coils [15].

The rotation observations were obtained from the Alcator C-Mod tokamak, a compact (major radius 0.67 m, minor radius 0.22 m), high magnetic field ($B_T \leq 8$ T) device with strong shaping capabilities and all metal plasma facing components. Auxilliary heating is available with up to 4 MW of ICRF heating power at 80 MHz. For the plasmas described here, the hydrogen minority heating was with $0 - \pi$ phasing, and there was no momentum input. Shown in Fig.1 are the time histories of the (impurity) toroidal rotation velocities at three radii and the rotation of magnetic perturbations in pre- and post-cursors of sawtooth oscillations, for a 2.0 MW ICRF heated EDA H-mode [25] plasma. This 0.8 MA, 5.3 T discharge entered EDA H-mode at 0.655 s,

as indicated by the drop in the D_α signal, with a subsequent increase in the plasma stored energy and toroidal rotation velocity [14]. The velocity increase was first seen

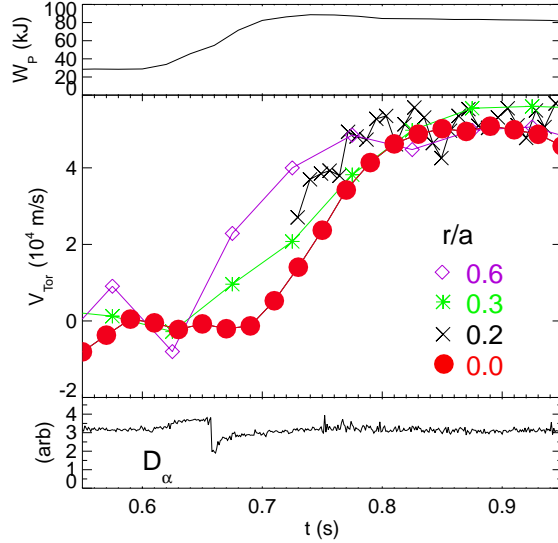


Figure 1: The plasma stored energy, impurity toroidal rotation velocity at three radii (red dots, green asterisks and purple diamonds for $r/a = 0.0, 0.3$ and 0.6 , respectively), magnetic perturbation rotation (\times s) at the sawtooth inversion radius ($r/a \sim 0.2$), and the edge D_α brightness for an ICRF heated EDA H-mode discharge.

on the outermost spectrometer ($r/a = 0.6$), sequentially moving inside, suggesting an edge source of toroidal momentum which propagated in towards the center, with a time scale somewhat longer than τ_E , the energy confinement time. After about 150 ms (0.8 s), the rotation settled to a value of ~ 50 km/s (in the co-current direction), with a flat profile. The fact that the rotation velocities for argon ions and $m=1$ perturbations are the same in steady state bolsters arguments from collisional coupling calculations that it is the bulk plasma rotation being measured [15]. During this steady phase of the discharge, the central electron density was $2.8 \times 10^{20}/\text{m}^3$ and the central electron temperature was 2.1 keV. Similar velocity profile evolution has been seen in purely Ohmic EDA H-mode plasmas without ICRF heating. This time evolution and flat steady state rotation profile suggest that the momentum transport in EDA H-mode plasmas may be characterized by a purely diffusive process. The situation is different in ELM-free H-mode plasmas, as can be seen in Fig.2. This 0.8 MA, 4.6 T discharge entered ELM-free H-mode at 0.624 s, reverted to L-mode at 0.834 s, then re-entered ELM-free H-mode at 0.871 s. Following both L-H transitions, there was a rapid increase in the core rotation velocity and stored energy. In contrast to the EDA H-mode case, these rotation profiles are highly peaked [14], reaching ~ 70 km/s in the core, in the absence of

external momentum input, and ~ 15 km/s at $r/a=0.6$. This demonstrates momentum transport up the velocity gradient and suggests the presence of an inward momentum pinch [11]. During the first ELM-free period, the central electron temperature was rel-

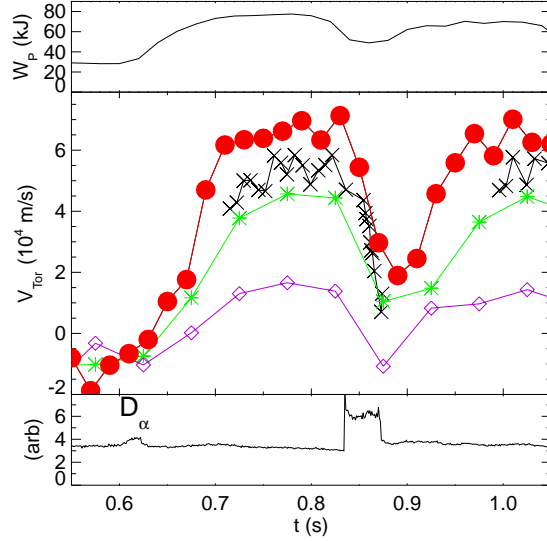


Figure 2: The plasma stored energy, impurity toroidal rotation velocity at three radii (red dots, green asterisks and purple diamonds for $r/a = 0.0, 0.3$ and 0.6 , respectively), magnetic perturbation rotation (\times) at the sawtooth inversion radius ($r/a \sim 0.2$), and the edge D_α brightness for an ICRF heated ELM-free H-mode discharge.

atively constant at 1750 eV, while the electron density rose continuously from 1.1 to $2.9 \times 10^{20}/\text{m}^3$, maintaining a flat profile. Improved particle and impurity confinement is a characteristic of ELM-free discharges; whether this momentum peaking is related is an open question. In contrast to these peaked rotation profiles are the hollow profiles which develop in internal transport barrier (ITB) plasmas. ITB discharges can be produced with off-axis ICRF heating [24,26], provided the resonance location is outside of $r/a = 0.5$, and that the plasma first enters EDA H-mode. These ITBs are characterized by a strong peaking of the core electron density which evolves in conjunction with a decrease and reversal of the core toroidal rotation velocity [24,26]. Shown in Fig.3 are the rotation time histories for a 4.5 T, 0.8 MA EDA H-mode plasma produced with 2.2 MW of off-axis ICRF heating power at 80 MHz. Up until 0.85 s, this plasma exhibited the normal EDA H-mode rotation characteristics (Fig.1) with the velocity propagating in from the outside, and the profile becoming flat across most of the plasma. After 0.85 s, the core rotation inside $r/a=0.5$ (the location of the barrier foot) dropped and reversed direction simultaneously with a strong peaking of the electron density profile also inside of $r/a=0.5$. The rotation at $r/a=0.6$, outside of the barrier foot, decreased

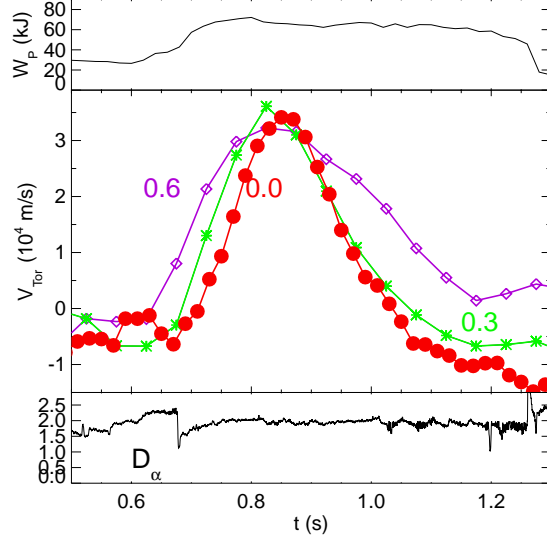


Figure 3: The plasma stored energy, impurity toroidal rotation velocity at three radii and the edge D_α brightness for an off-axis ICRF heated ITB discharge.

more slowly and not so far, indicating a positive velocity gradient in the vicinity of the ITB foot. The radial electric field, E_r , determined from the force balance equation and from calculations of the poloidal magnetic field, assuming neo-classical poloidal velocity, was found to be -10 kV/m at $r/a=0.3$ (inside of the ITB foot) and $+5$ kV/m at $r/a=0.6$ (outside of the foot), and a lower limit of the E_r gradient is ~ 250 kV/m² at 1.1 s.

The evolution of the velocity profile has been simulated using a simple source-free momentum transport model

$$\frac{\partial}{\partial t}P + \nabla \cdot \left(-D_\phi \frac{\partial}{\partial r}P - \frac{v_c r}{a}P \right) = 0 \quad (1)$$

with $P = n_i m_i V_\phi$, where a is the minor radius and where the momentum diffusivity, D_ϕ , and the momentum convection velocity, v_c , are free parameters to be determined. In cylindrical coordinates and subject to the boundary conditions of an edge rotation, V_0 , during H-mode

$$V_\phi(a, t) = \begin{cases} 0, & t < t_{L \rightarrow H} \\ V_0, & t_{L \rightarrow H} \leq t \leq t_{H \rightarrow L} \\ 0, & t > t_{H \rightarrow L} \end{cases} \quad (2)$$

and with the assumptions (observed in the electrons) of a flat ion density profile, and

spatially and temporally constant D_ϕ and v_c , the toroidal rotation velocity, V_ϕ , profile evolution may be determined from a solution to

$$\frac{\partial}{\partial t} V_\phi - D_\phi \left[\frac{\partial^2}{\partial r^2} V_\phi + \left(\frac{1}{r} + \frac{v_c r}{a D_\phi} \right) \frac{\partial}{\partial r} V_\phi + \frac{2v_c}{a D_\phi} V_\phi \right] = 0 \quad (3)$$

via an expansion in confluent hypergeometric functions.

An example of a comparison of this model to the observed velocity time evolution in an EDA H-mode plasma similar to that presented in Fig.1 is shown in the top frame of Fig.4. The time of the L- to H-mode transition was 1.11 s. The three curves

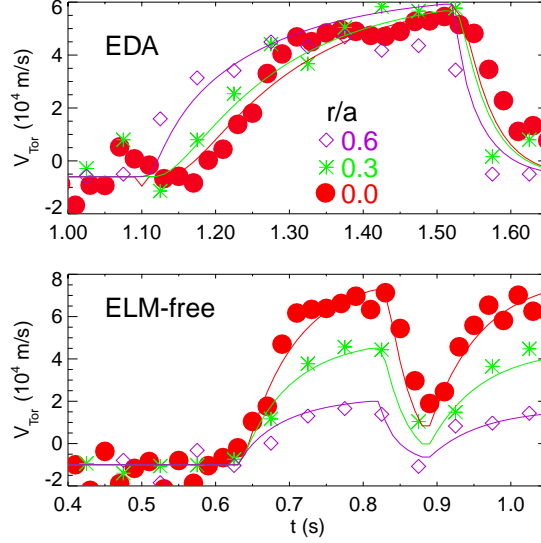


Figure 4: Comparison of model calculations (solid lines) with observed rotation time histories for an EDA H-mode plasma (top frame) and an ELM-free H-mode plasma (bottom frame).

represent the simulated rotation velocities at the radii of the three spectrometer views. For this case, D_ϕ was spatially constant with a value of $0.05 \text{ m}^2/\text{s}$, and $v_c \approx 0$, which corresponds to a momentum confinement time, τ_ϕ , of 150 ms. This momentum diffusivity is much greater than the neo-classical viscosity, $\chi_\phi \sim \rho_i^2 / \tau_{ii} \sim 0.003 \text{ m}^2/\text{s}$ for this case, and the momentum transport may be characterized as anomalous. The momentum diffusivity may also be determined for L-mode from the decay of the rotation velocity after the H- to L-mode transition at 1.53 s; D_ϕ for the L-mode portion of this discharge was $0.20 \text{ m}^2/\text{s}$, with $\tau_\phi \sim 35$ ms. From modeling of several ICRF and Ohmic EDA H-mode plasmas, D_ϕ was found to be in the range from 0.05 to $0.10 \text{ m}^2/\text{s}$, with $v_c \approx 0$. The simulations for the ELM-free discharge from Fig.2 are shown in the bottom frame of Fig.4, which is on the same time scale as the top frame for comparison. In this

instance D_ϕ was $0.40 \text{ m}^2/\text{s}$ with $v_c = 12 \text{ m/s}$, and $\tau_\phi \sim 70 \text{ ms}$. This value of the pinch velocity was necessary to match the quasi-steady peaked profile shape at 0.8 s , with a ‘peaking factor’, $S \equiv av_c/2D_\phi = 3.2$, along with the overall rise time of the rotation. From the rotation decay after the H- to L-mode transition, a value of $D_\phi \sim 0.25 \text{ m}^2/\text{s}$ was determined. From the rotation decays in many discharges after the H- to L-mode transition, D_ϕ for L-mode was determined to be in the range from $0.20\text{-}0.25 \text{ m}^2/\text{s}$, with $v_c = 0$.

The model of Eq.(3) cannot be strictly applied to the ITB case in Fig.3 because the electron (ion) and argon density profiles [26] were peaking in the core during the barrier evolution. However, along with the negative rotation velocity inside of the barrier foot, this implies a negative momentum density in the core, which would require an outward momentum convection in the core during the ITB phase.

In the progression from L-mode to EDA H-mode to ELM-free H-mode to ITB discharges, the particle diffusivity steadily drops (particle confinement increases), approaching neo-classical levels in the core in ITB plasmas. EDA H-mode plasmas have temporally and spatially constant electron density profiles, ELM-free H-mode plasmas exhibit steadily rising electron density profiles which maintain a flat shape and ITB discharges show a central peaking of the density profile [24,26] consistent with the neo-classical Ware pinch velocity. The same sequence of impurity confinement may be characterized as highly anomalous in L-mode, with an impurity diffusivity $D_I \sim 0.5 \text{ m}^2/\text{s}$ ($\tau_I \sim 15\text{-}25 \text{ ms}$) and $D_I \sim 0.1\text{-}0.3 \text{ m}^2/\text{s}$ in EDA H-mode with $\tau_I \sim 50\text{-}150 \text{ ms}$ [27]. For ELM-free H-mode plasmas, the impurity confinement is long ($\tau_I \sim 1 \text{ s}$) with reduced D_I ($\sim 0.05 \text{ m}^2/\text{s}$) and substantial inward convection ($10\text{-}100 \text{ m/s}$) at the edge [27]. In ITB discharges there is strong core impurity accumulation [26] with D_I ($\sim 0.02 \text{ m}^2/\text{s}$) and v_I ($\sim 100 \text{ ms}$ inward) close to the neo-classical values in the core plasma. Energy confinement exhibits a somewhat similar progression with χ_{eff} dropping from $\sim 1 \text{ m}^2/\text{s}$ in L-mode, to $\sim 0.5 \text{ m}^2/\text{s}$ in H-mode [25] and then as far as $\sim 0.1 \text{ m}^2/\text{s}$ (near the neo-classical level) in the core plasma during ITB [26] operation. Momentum confinement demonstrates some similarities in behavior; there is a decrease in the momentum diffusivity from $0.20\text{-}0.25 \text{ m}^2/\text{s}$ in L-mode to the range $0.05\text{-}0.10 \text{ m}^2/\text{s}$ in EDA H-mode. Also, in ELM-free H-mode there is a strong momentum pinch, with $v_c \sim 10 \text{ m/s}$, analogous to the observations of impurity transport. In ITB discharges, particle, impurity and energy confinement may be characterized by transport coefficients with values similar to neo-classical levels in the core. For these discharges, however, the momentum seems to be expelled from the plasma center, rather than having increased confinement. The reason that the momentum transport in ITB discharges doesn’t follow the behavior of particle and energy confinement may be because these plasmas have a negative E_r well in the core, and may be influenced by the fact that momentum is an odd moment of the distribution function, having directionality.

The momentum transport in C-Mod has been found to be anomalous, with momentum diffusivities much larger than neo-classical levels. The cause of the toroidal rotation, generated in the absence of a momentum source, as well as the varying velocity profile shapes, remains unexplained.

The authors thank A. Hubbard for T_e measurements, S. Wolfe for magnetic equi-

librium calculations, J. Terry for D_α measurements, P. Bonoli and S. Scott for useful discussions, S. Wukitch and Y. Lin for operation of the ICRF systems and J. Irby and the Alcator C-Mod operations group for expert running of the tokamak. Work supported at MIT by DoE Contract No. DE-FC02-99ER54512.

References

- [1] K.C.Shaing and E.C.Crume, Phys. Rev. Lett. **63** (1989) 2369.
- [2] H.Biglari et al., Phys. Fluids **B2** (1990) 1.
- [3] R.J.Groebner et al., Phys. Rev. Lett. **64** (1990) 3015.
- [4] K.Ida et al., Phys. Rev. Lett. **65** (1990) 1364.
- [5] K.Burrell, Phys. Plasmas **4** (1997) 1499.
- [6] S.Suckewer et al., Nucl. Fusion **21** (1981) 1301.
- [7] K.H.Burrell et al., Nucl. Fusion **28** (1988) 3.
- [8] S.D.Scott et al., Phys. Rev. Lett **64** (1990) 531.
- [9] A.Kallenbach et al., Plasma Phys. Contr. Fusion **33** (1991) 595.
- [10] N.Asakura et al., Nucl. Fusion **33** (1993) 1165.
- [11] K.Nagashima et al., Nucl. Fusion **34** (1994) 449.
- [12] K.-D.Zastrow et al., Nucl. Fusion **38** (1998) 257.
- [13] J.S.deGrassie et al., Nucl. Fusion **43** (2003) 142.
- [14] J.E.Rice et al., Nucl. Fusion **38** (1998) 75.
- [15] I.H.Hutchinson et al., Phys. Rev. Lett. **84** (2000) 3330.
- [16] L.-G.Eriksson et al., Plasma Phys. Contr. Fusion **39** (1997) 27.
- [17] I.H. Coffey, R. Barnsley, F.P. Keenan *et al.*, in Proceedings of the 11th Colloquium on UV and X-ray Spectroscopy of Astrophysical and Laboratory Plasmas, Nagoya, Japan, 1995, p.431, Frontiers Science Series No.15 (Editors: K. Yamashita and T. Watanabe), Universal Academy Press, Tokyo, Japan, 1996
- [18] G.T.Hoang et al., Nucl. Fusion **40** (1999) 913.
- [19] F.W.Perkins, et al., Phys. Plasmas **8** (2001) 2181.
- [20] L.-G.Eriksson and F.Porcelli, Nucl. Fusion **42** (2002) 959.
- [21] K.C.Shaing, Phys. Rev. Lett. **86** (2001) 640.
- [22] B.Coppi, Nucl. Fusion **42** (2002) 1.
- [23] A.L.Rogister, et al., Nucl. Fusion **42** (2002) 1144.
- [24] J.E.Rice et al., Nucl. Fusion **41** (2001) 277.
- [25] M.Greenwald et al., Nucl. Fusion **37** (1997) 793.
- [26] J.E.Rice et al., Nucl. Fusion **42** (2002) 510.
- [27] J.E.Rice et al., Phys. Plasmas **4** (1997) 1605.